The role of outer rainband convection in governing the eyewall replacement cycle in numerical simulationed of tropical cyclones

Zhenduo Zhu and Ping Zhu

Department of Earth and Environment, Florida International University, Miami, Florida, USA

JGR 2014

Introduction

- The eyewall replacement cycle (ERC) is a common phenomenon often in major tropical cyclones (TCs) that may cause serious dramatic intensity and structure changes of the storm.

- 4 mechanism of secondary eyewall formation (SEF):
  - dynamic adjustment to latent heating outside the primary eyewall
  - asymmetric vortex interaction via axisymmetrization
  - radiation of vortex Rossby waves and the wave-mean flow interaction near the critical radius
  - unbalanced dynamics associated with boundary layer (BL) processes.

Introduction

- The sustained azimuthal mean latent heating outside the primary eyewall eventually leads to SEF facilitated by a broadening wind field, which enhances the frictional inflow and the inertial stability. (Rozoff et al., 2012)

- The rainband convective activities can accumulate the potential vorticity (secondary wind maximum) in the outer eyewall region. (Judt and Chen, 2010; Moon and Nolan, 2010)

- Enhanced latent heating favors the outward expansion of winds and SEF. (Wang 2009)

- The shear effect can have a substantial impact on the asymmetric latent heating that promotes SEF. (Fang and Zhang, 2012)

Introduction

- A concentric vorticity structure can result from the interaction between a small strong inner vortex and asymmetric neighboring weak vortices through the axisymmetrizing process. (Kuo et al.,2004, 2008)

- The negative radial vorticity gradient outside RMW supports the outward propagating VRWs until the waves slow down approaching the stagnation radius where the group velocity of VRWs goes to zero. The maximum acceleration of tangential wind generated by wave-meanflow interaction at that radius. (Montgomery and Kallenbach, 1997; Martinez et al., 2010; Menelaou et al., 2013)

Introduction

- Unbalanced BL processes: broadening of the tangential winds→increasing of BL inflow→ developing of convergence zone (supergradient wind) within and above the BL

- The convergence zone initiate the eruption of moist air out of the BL to foster deep convection that forms the root of secondary eyewall. (Huang et al., 2012)

- The BL dynamics alone is capable of developing secondary wind maxima by an axisymmetric nonlinear slab BL model. (Abarca and Montgomery, 2013)

- It is unclear if the broadening of the tangential winds is the cause for initiating a SEF or the outcome of an initiated SEF by other processes.

Introduction

- Demising of the inner eyewall might be caused by a disruption of its transverse circulation during the contraction and intensification of the outer eyewall. The outer eyewall cut off the BL inflow into the inner eyewall. (Willoughby et al., 1982)

- As the outer eyewall intensifies and moves inward, the subsidence of the deep convection in the outer eyewall could inhibit the updraft in the inner eyewall region. (Willoughby et al., 1982; and Willoughby 1990)

- This paper:
  - the physical processes leading to the formation and development of the secondary maximum of tangential wind associated with the outer eyewall
  - the mechanism of the demise of inner eyewall
  - in the 3-D full physics WRF simulations

WRF Configuration

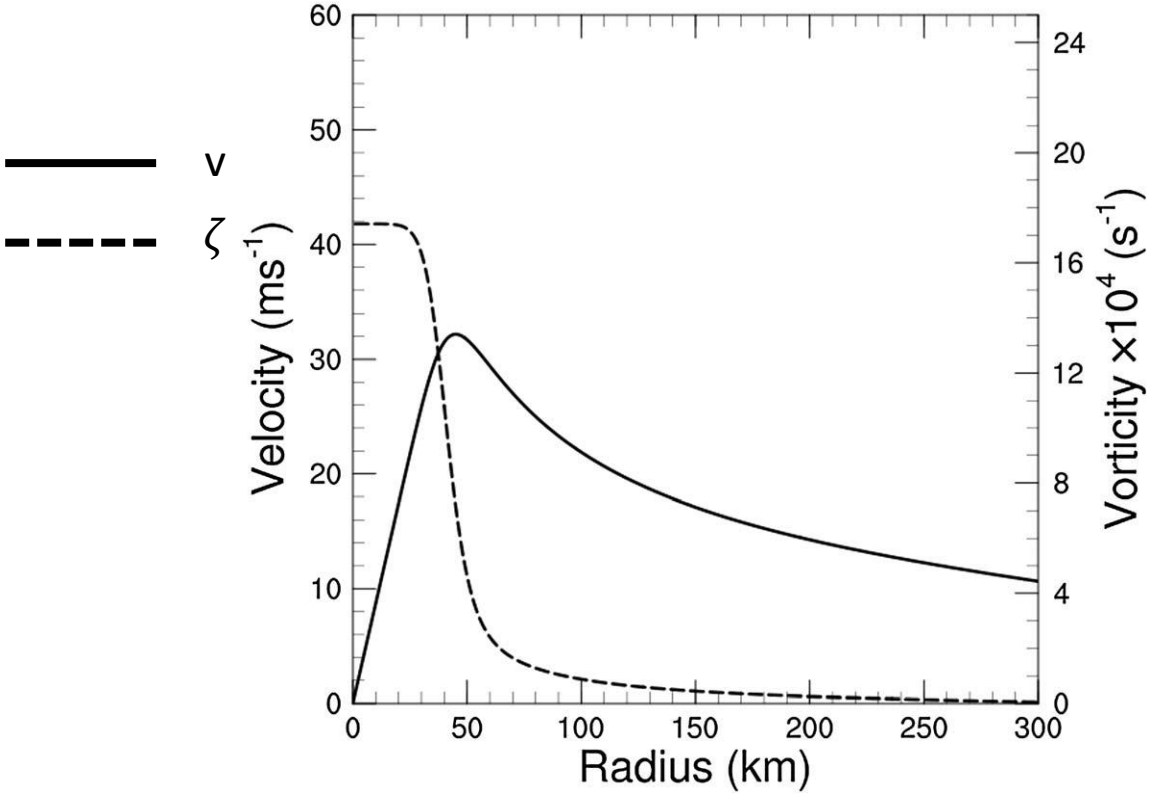

- Surface RMW: 45 km
- Max wind: 36 m/s

Vertical:

$$\overline{v}(r,\ z) = \overline{V}(r)\ \exp\left\{-\left(\frac{cz}{z_{\text{top}}}\right)^{\alpha}\right\}$$

$$\times\left[1 - \gamma\ \exp\left\{-\left(\frac{r}{\delta + \kappa z}\right)^{\beta}\right\}\right]$$

Version	3.3.1
Domains	3
Grid size	18, 6, 2 (km)
Run time	8 days
Eta levels	47 (higher resolution in BL and upper troposphere)
Model top	20 hPa
West/East B.C	Periodic
North/South B.C.	Free-slip
Cumulus Scheme	Kain-Fritch (d01 only)
Microphysics Scheme	Thompson
Longwave Scheme	RRTM
Shortwave Scheme	Dudhia
PBL Scheme	MYJ
SST	29°C (open ocean)
Others	f-plane (20°N)

Overview of the simulation result

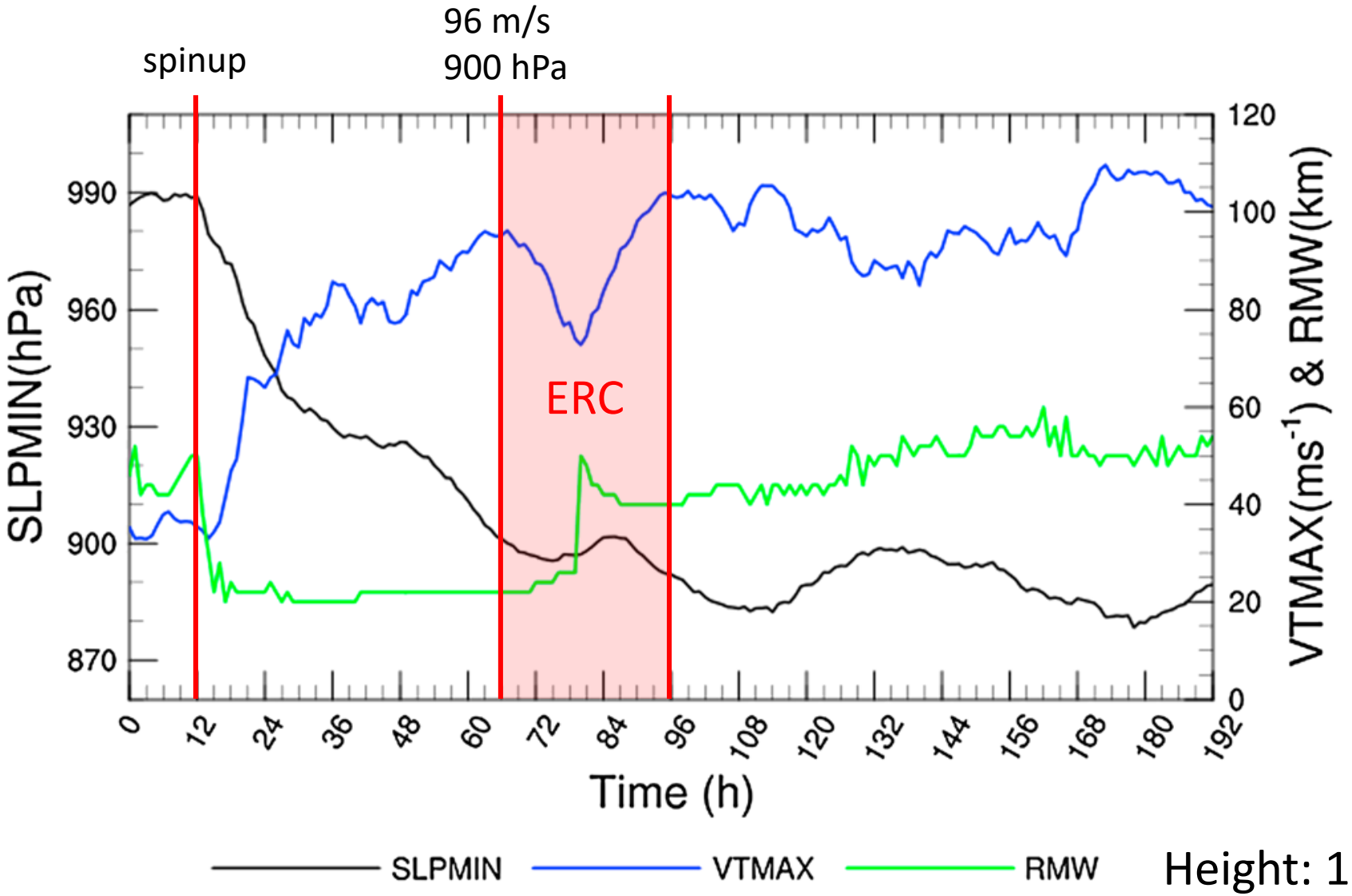

Height: 1 km

Simulation result

Height: 1 km
color: dBZ
black line: per 30 km

Plotting time (h):

56	58	60	62
64	66	68	70
72	74	76	78
80	82	84	86

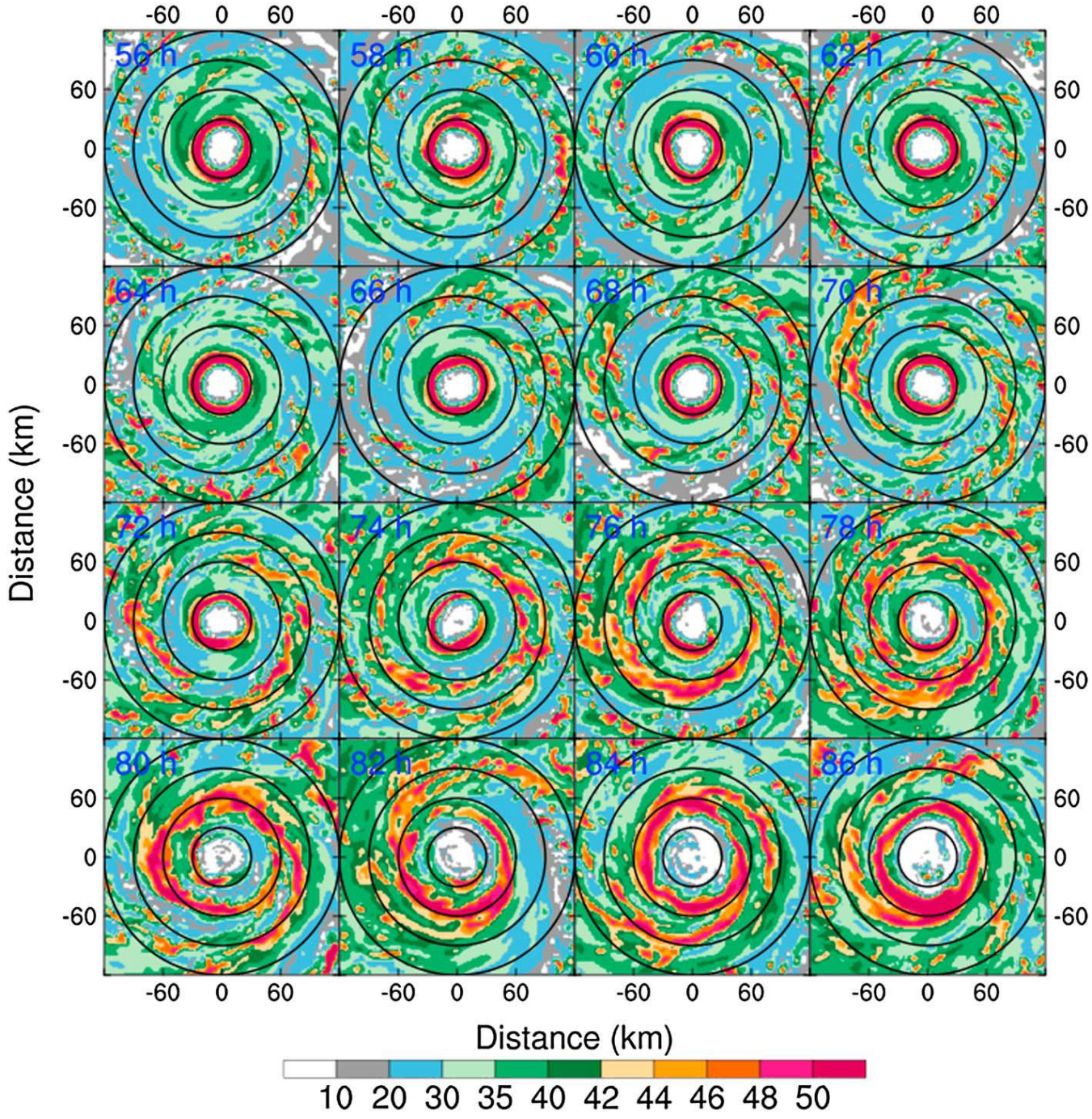

Simulation result

Axisymmetric
Hovmoller diagram

Left:
w at z = 5 km
Right:
v at z = 1 km

ERC features:
2nd Vmax
weakness of vortex
reintensification after ERC
larger RMW

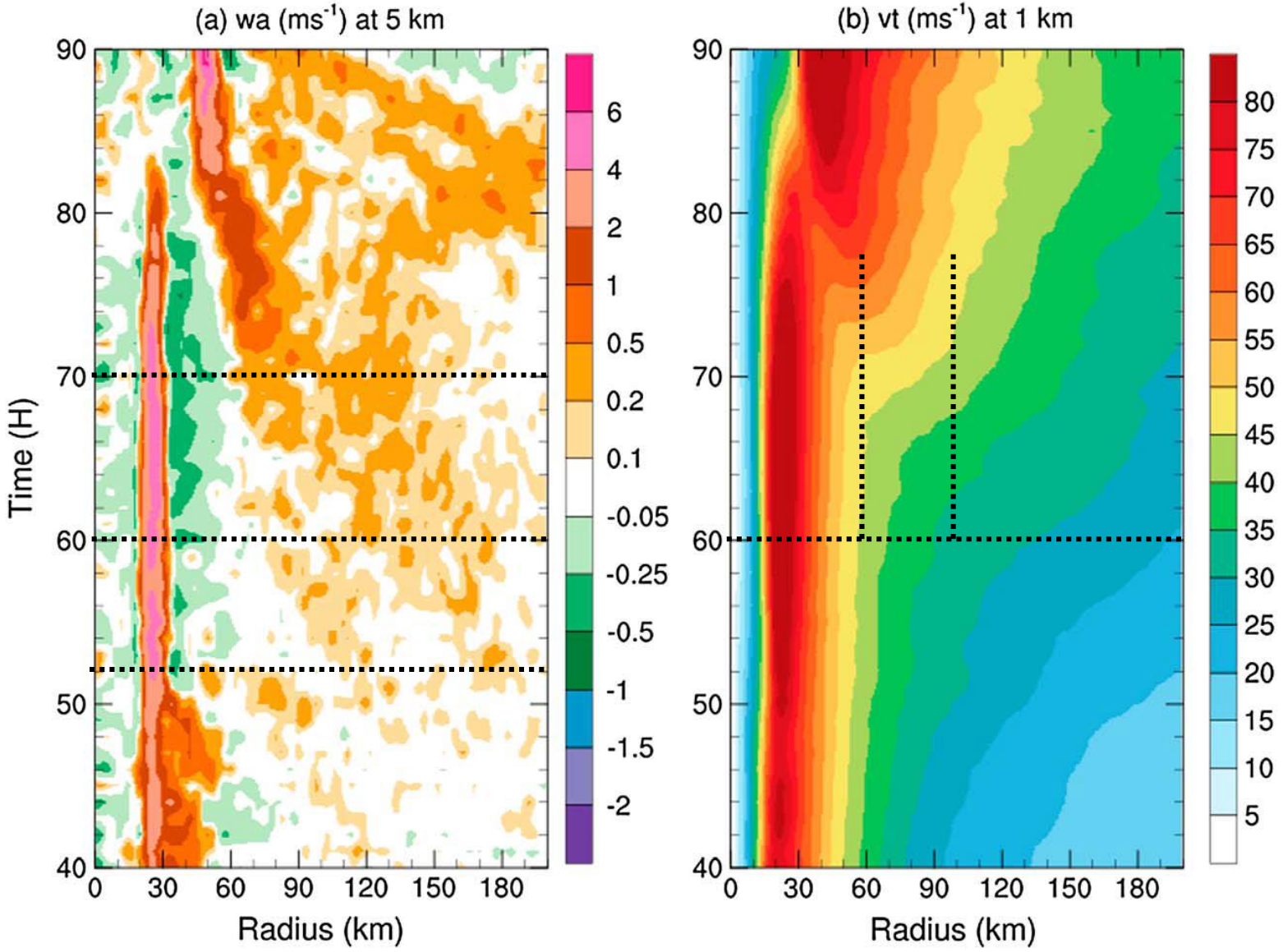

Evolution of 2nd max of tangential wind

Axisymmetric V

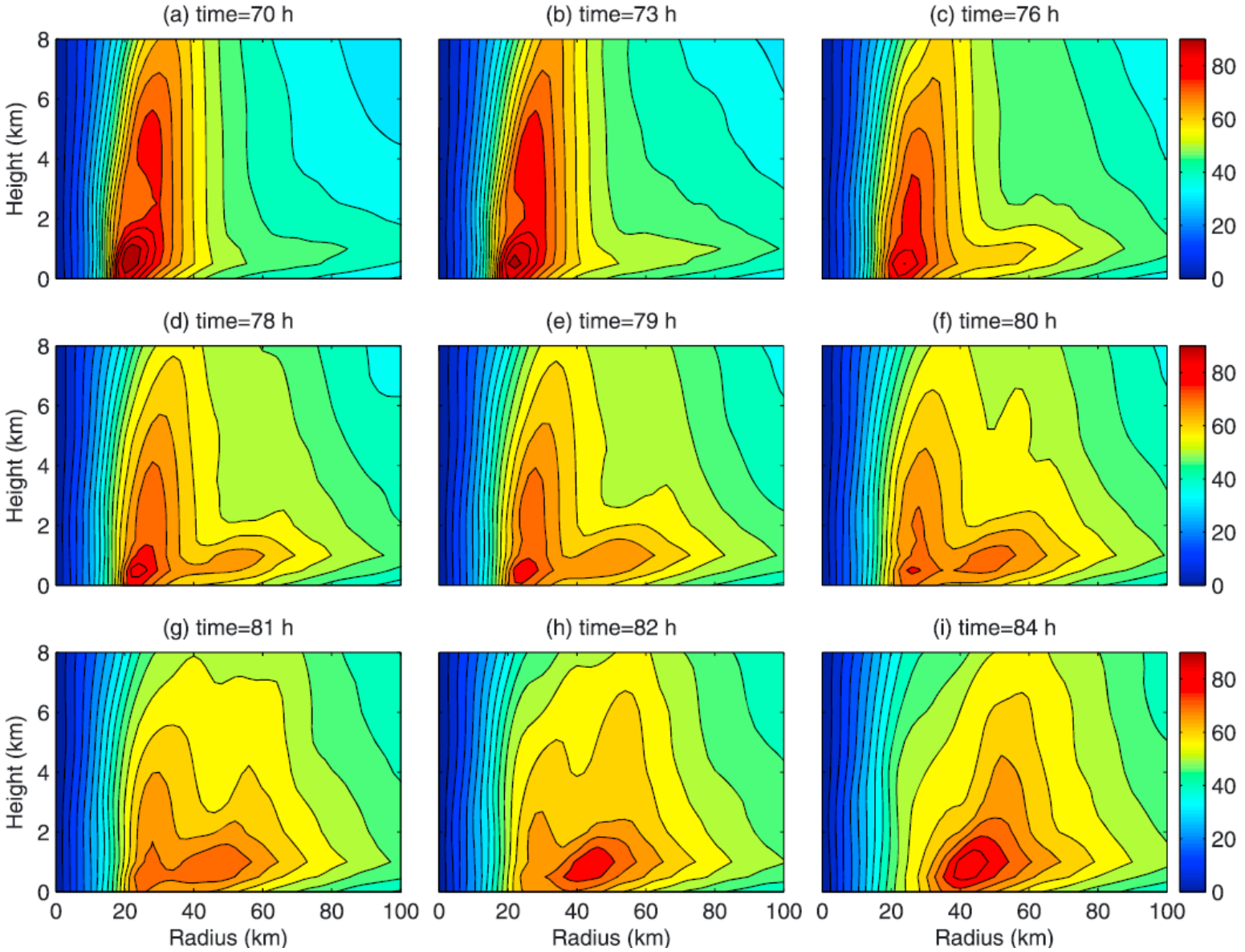

Tangential momentum budget

Axisymmetric
average of 79 ~ 81 h

Contour: $\overline{w}$

$$\frac{\partial \bar{v}}{\partial t} = -\bar{u}\overline{\zeta_a} - \bar{w}\frac{\partial \bar{v}}{\partial z}$$

$$-\overline{u'\zeta_a'} - \overline{v'\frac{\partial v'}{r\partial \lambda}} - \overline{w'\frac{\partial v'}{\partial z}} + \overline{TSGS_v}$$

$\overline{TSGS_v}$: vertical and horizontal diffusion
Time interval between 2 wrfout: 10 min

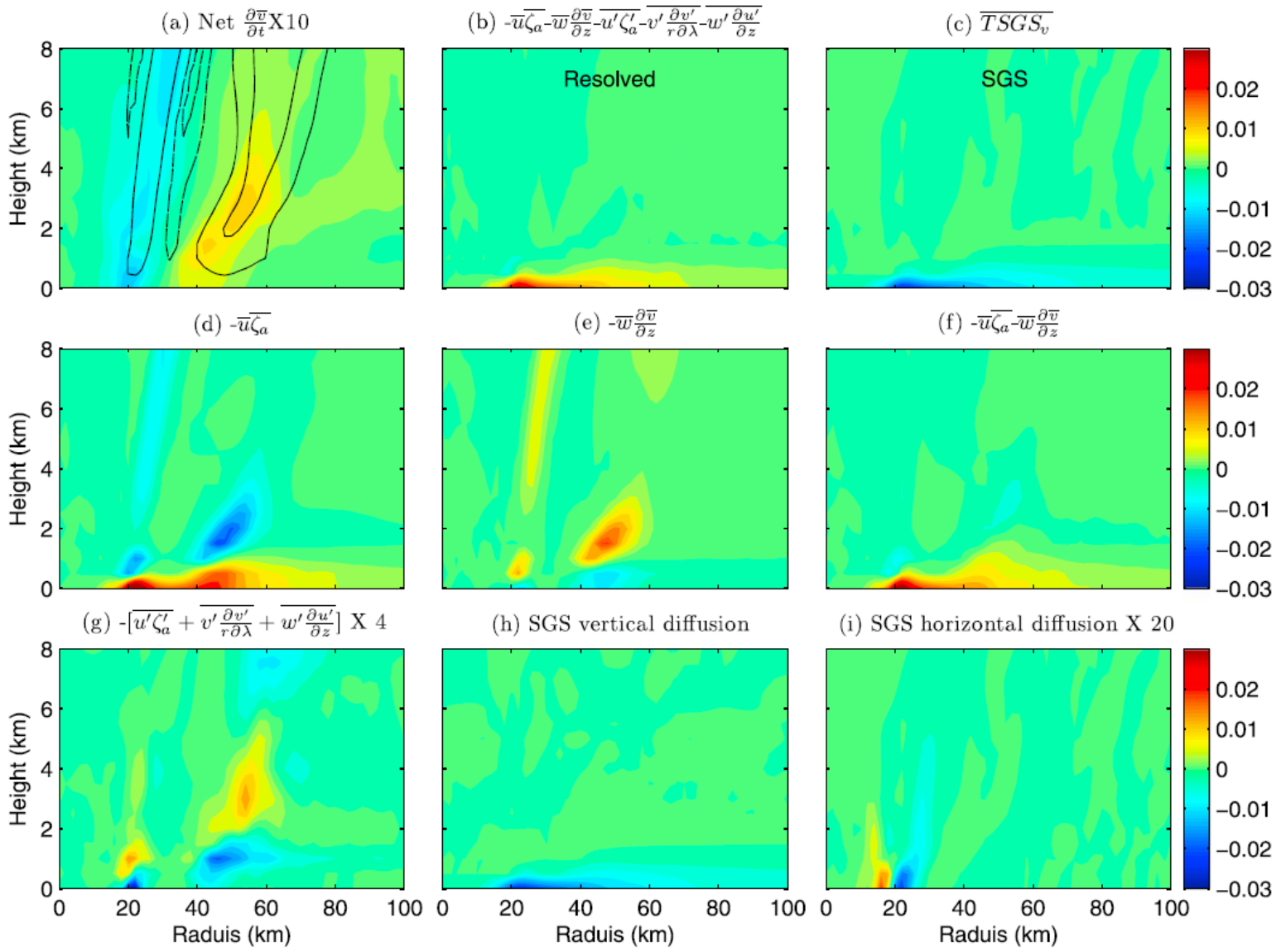

Sawyer-Eliassen Equation

$$\frac{\partial}{\partial r}\left[-g\frac{\partial\bar{\chi}}{\partial z}\frac{1}{r\rho_0}\frac{\partial\bar{\psi}}{\partial r}-\frac{\partial\bar{\chi}\bar{C}}{\partial z}\frac{1}{r\rho_0}\frac{\partial\bar{\psi}}{\partial z}\right]+\frac{\partial}{\partial z}\left[\left(\bar{\xi}\bar{\chi}(\bar{\zeta}+f)+\bar{C}\frac{\partial\bar{\chi}}{\partial r}\right)\frac{1}{r\rho_0}\frac{\partial\bar{\psi}}{\partial z}-\frac{\partial\bar{\chi}\bar{C}}{\partial z}\frac{1}{r\rho_0}\frac{\partial\bar{\psi}}{\partial r}\right]$$
$$=g\frac{\partial}{\partial r}(\bar{\chi}^2\bar{Q})+\frac{\partial}{\partial z}(\bar{C}\bar{\chi}^2\bar{Q})-\frac{\partial}{\partial z}(\bar{\chi}\bar{\xi}\bar{F}_\lambda)$$

Domain:

250 km in the horizontal
18 km in vertical

Assumption:

axisymmetric vortex
gradient-wind balance
hydrostatic balance

Boundary conditions:

$\psi = 0$ at the top, bottom and center

$\frac{\partial\bar{\psi}}{\partial r} = 0$ at $r = 250\ km$

$$\bar{F}_\lambda = -\overline{u'\zeta'_a} - v'\frac{\partial v'}{r\partial\lambda} - w'\frac{\partial v'}{\partial z} + \overline{TSGS_v},$$

$$\bar{Q} = \bar{\dot{\theta}} + \overline{u'\frac{\partial\theta'}{\partial r}} + \overline{v'\frac{\partial\theta'}{r\partial\lambda}} + \overline{w'\frac{\partial\theta'}{\partial z}} + \overline{TSGS_\theta},$$

Sawyer-Eliassen Equation

Heating profile
write plot: PV

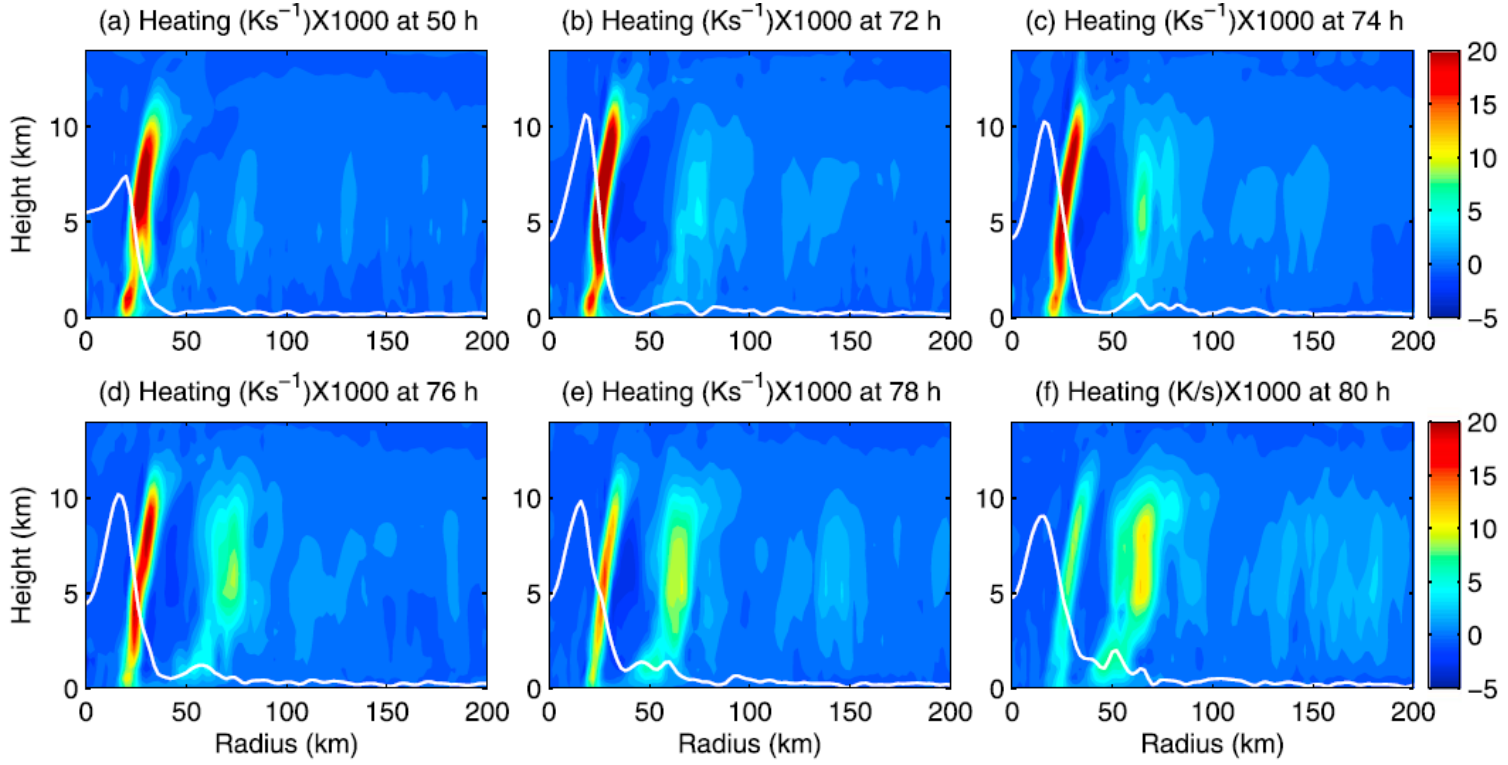

Time-Height
Diabatic heating
r = 60 ~ 80 km (SEF region)

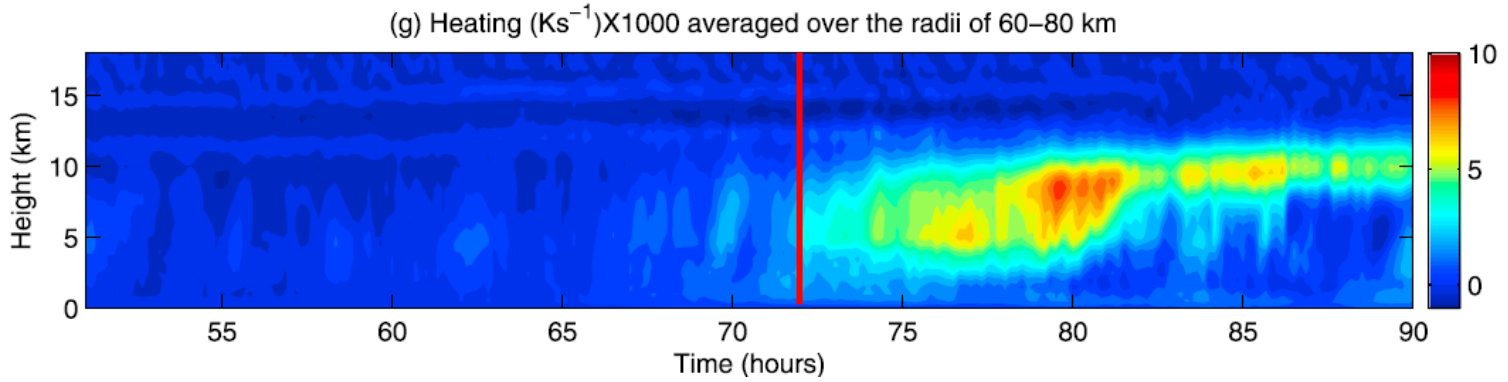

Sawyer-Eliassen Equation

(79 hr)

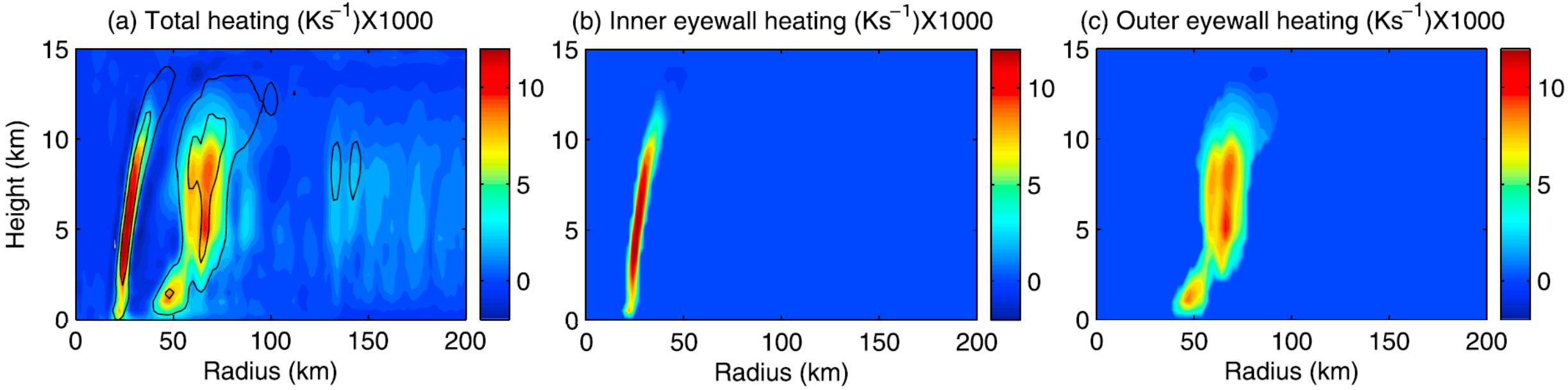

Contour: w > 0.5 m/s

Color: diabatic heating

Sawyer-Eliassen diagnose

Eyewall momentum
Eyewall heating
Rainband momentum
Rainband heating

$\bar{v}$ tendency at 1 km

$$\frac{\partial \bar{v}}{\partial t} \approx -\bar{u}\bar{\zeta}_a - \bar{w}\frac{\partial \bar{v}}{\partial z}$$

($\bar{u}$ and $\bar{w}$ are from S-E diagnose)

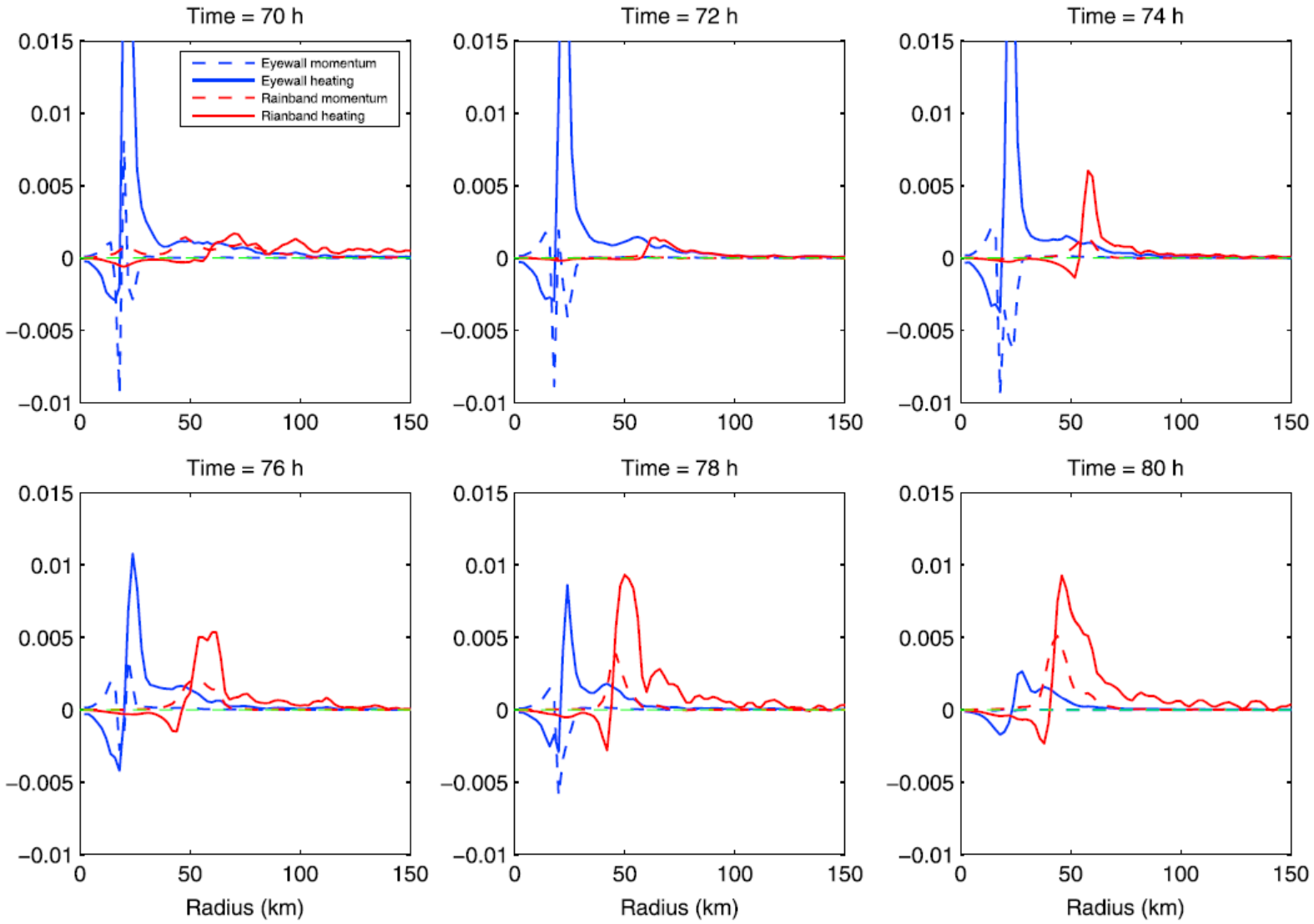

Sawyer-Eliassen diagnose

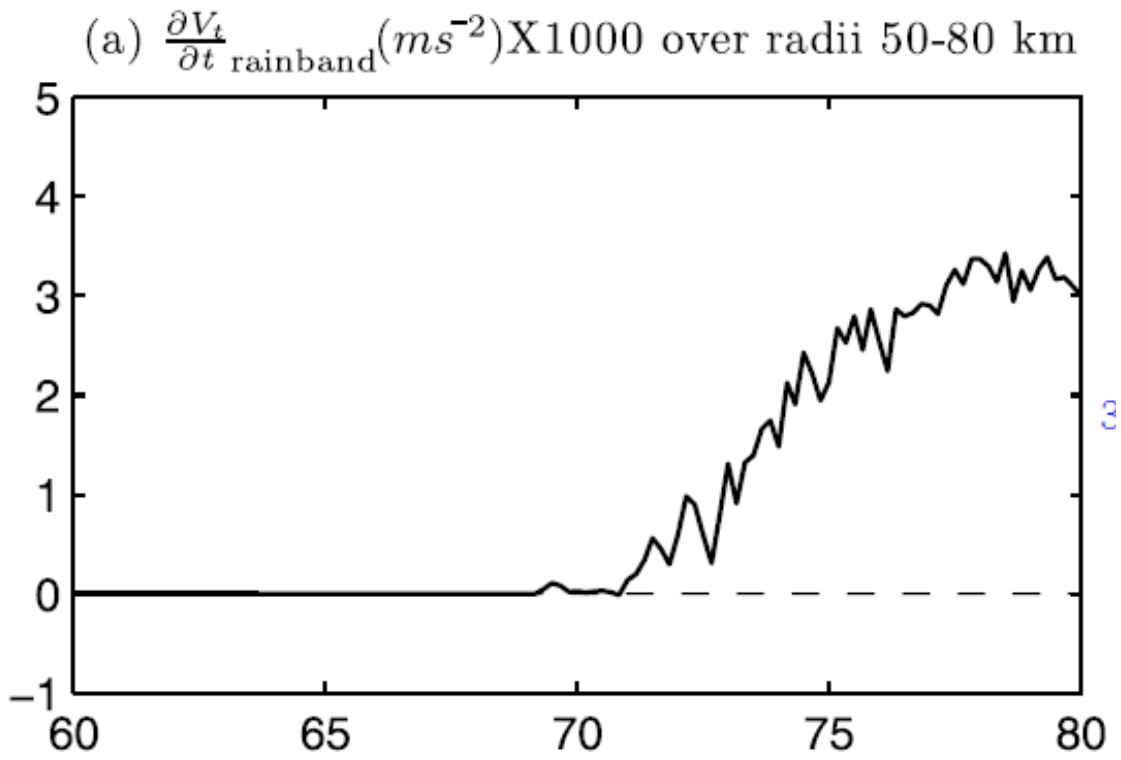

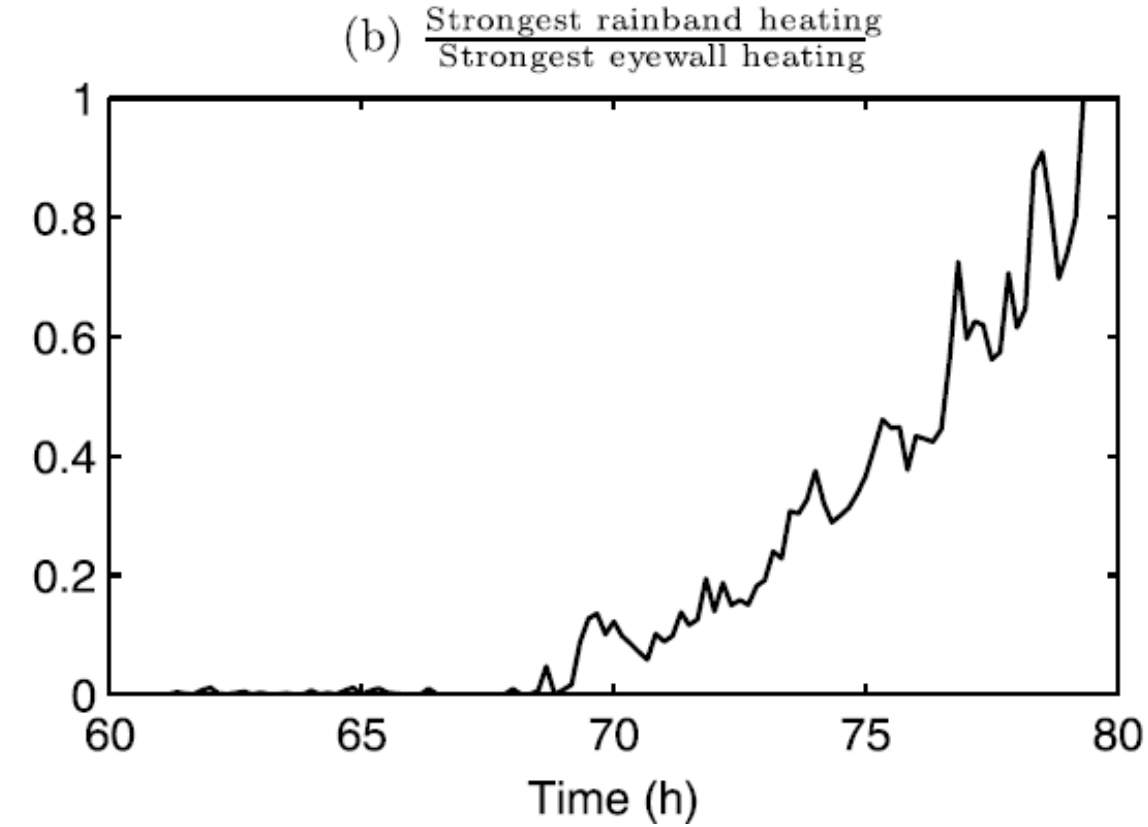

$\bar{v}$ tendency at 1 km
average along r = 50-80

$$\frac{Max(rainband\ heating)}{Max(eyewall\ heating)}$$

Sawyer-Eliassen diagnose

Outer rainband heating

$\bar{v}$ tendency

$\bar{u}$ divergence

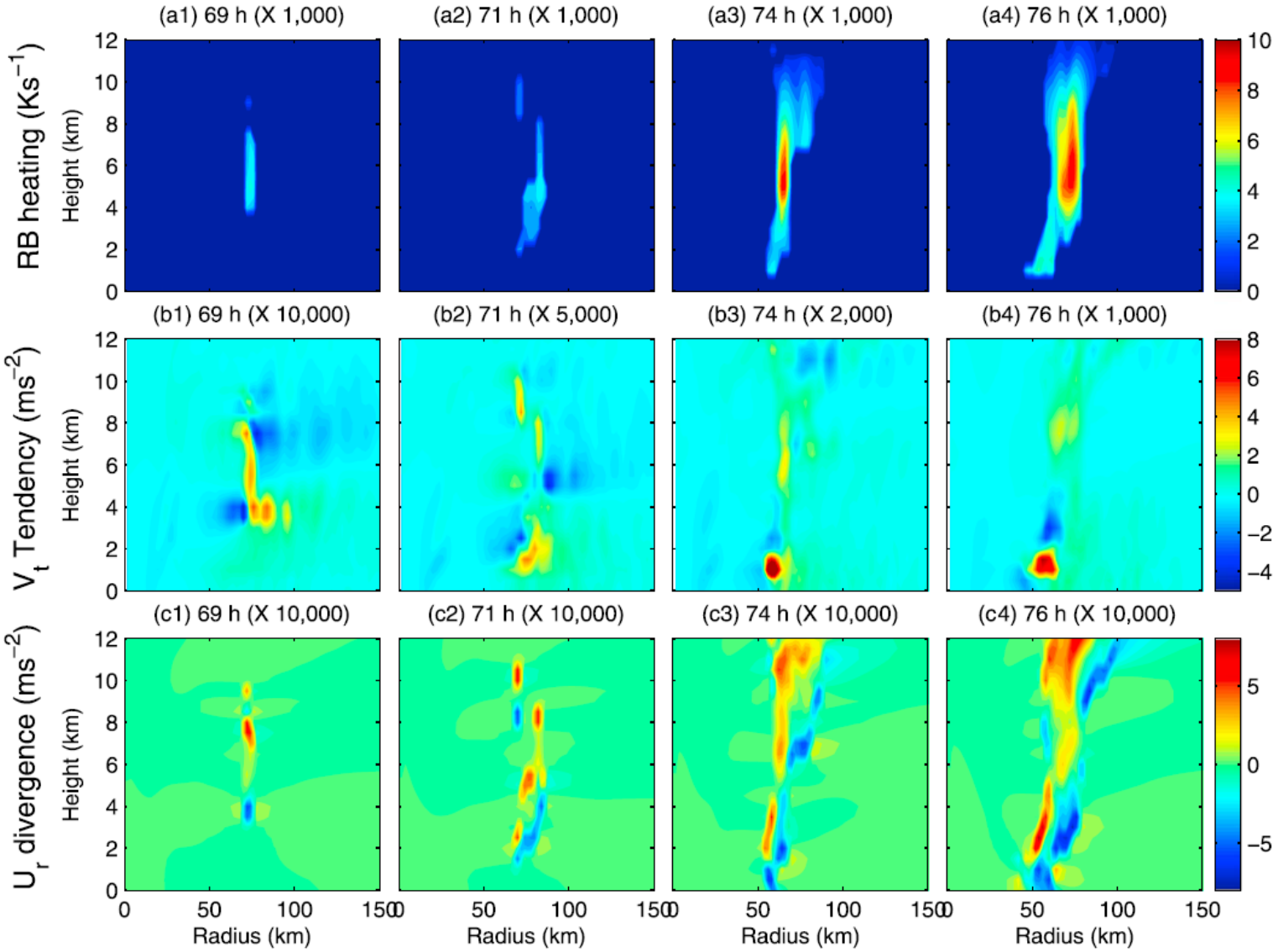

Sawyer-Eliassen diagnose

Outer eyewall heating

Outer rainband heating without heating below 3 km

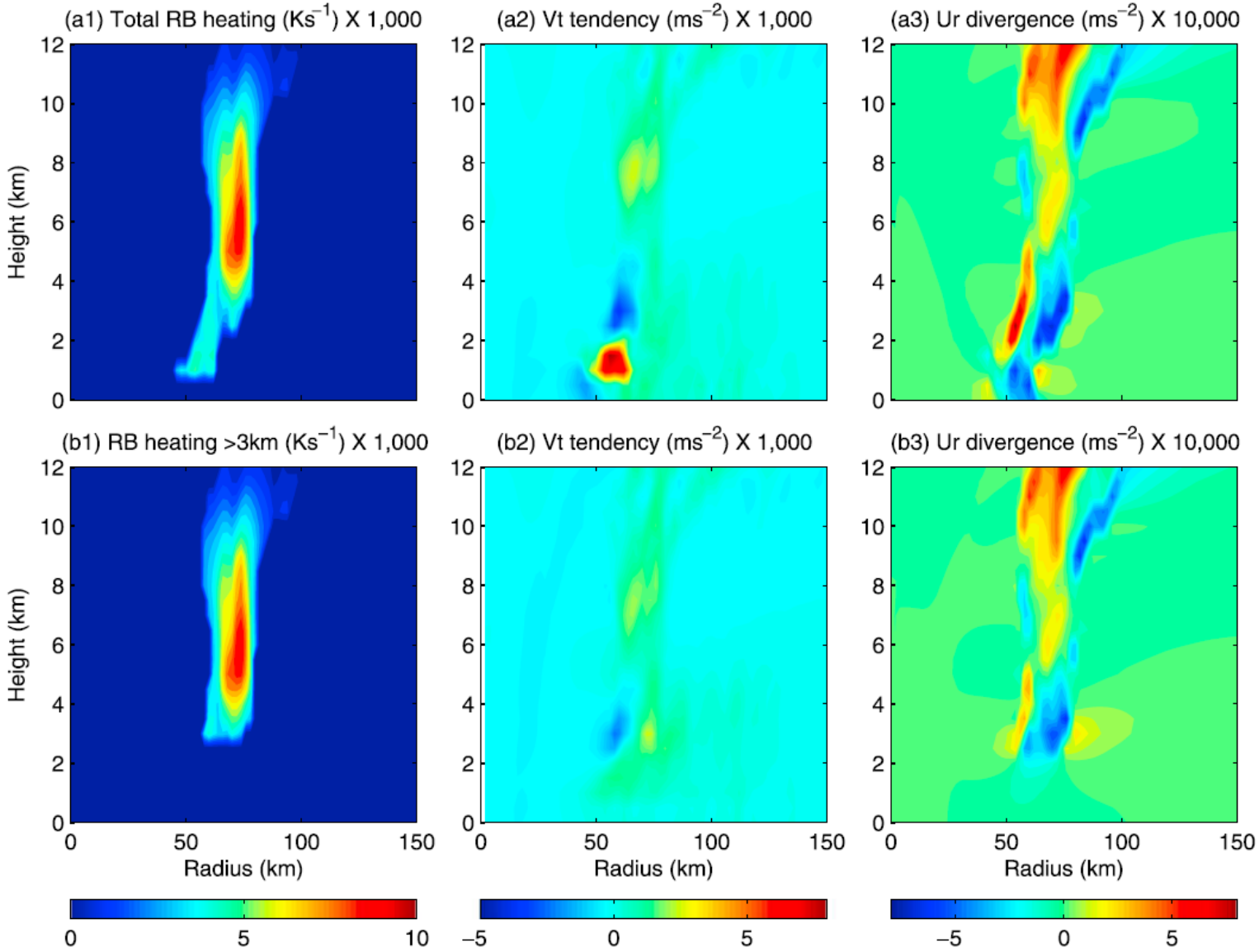

The mechanism of outer rainband convection

Sporadic convection occurs in the outer rainband region at mid-level.

The convergence of $\bar{u}$ and acceleration of $\bar{v}$ are generated at the convection base.

The moisture increases in the lower level.

Convection occurs at lower level.

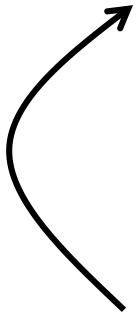

The mechanism of outer rainband convection

Average along
r = 50 ~ 80 km

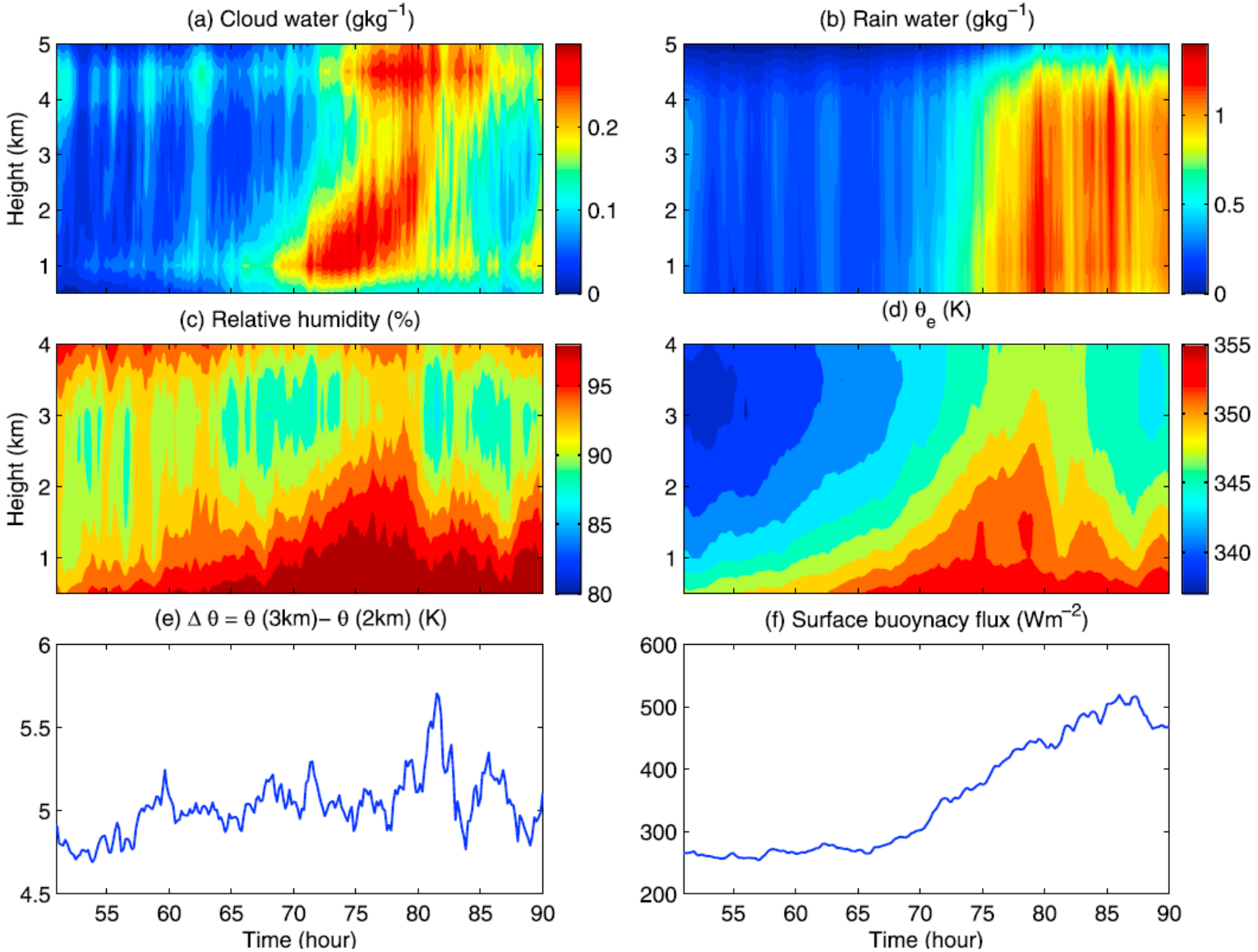

Interaction between eyewalls & RB during ERC

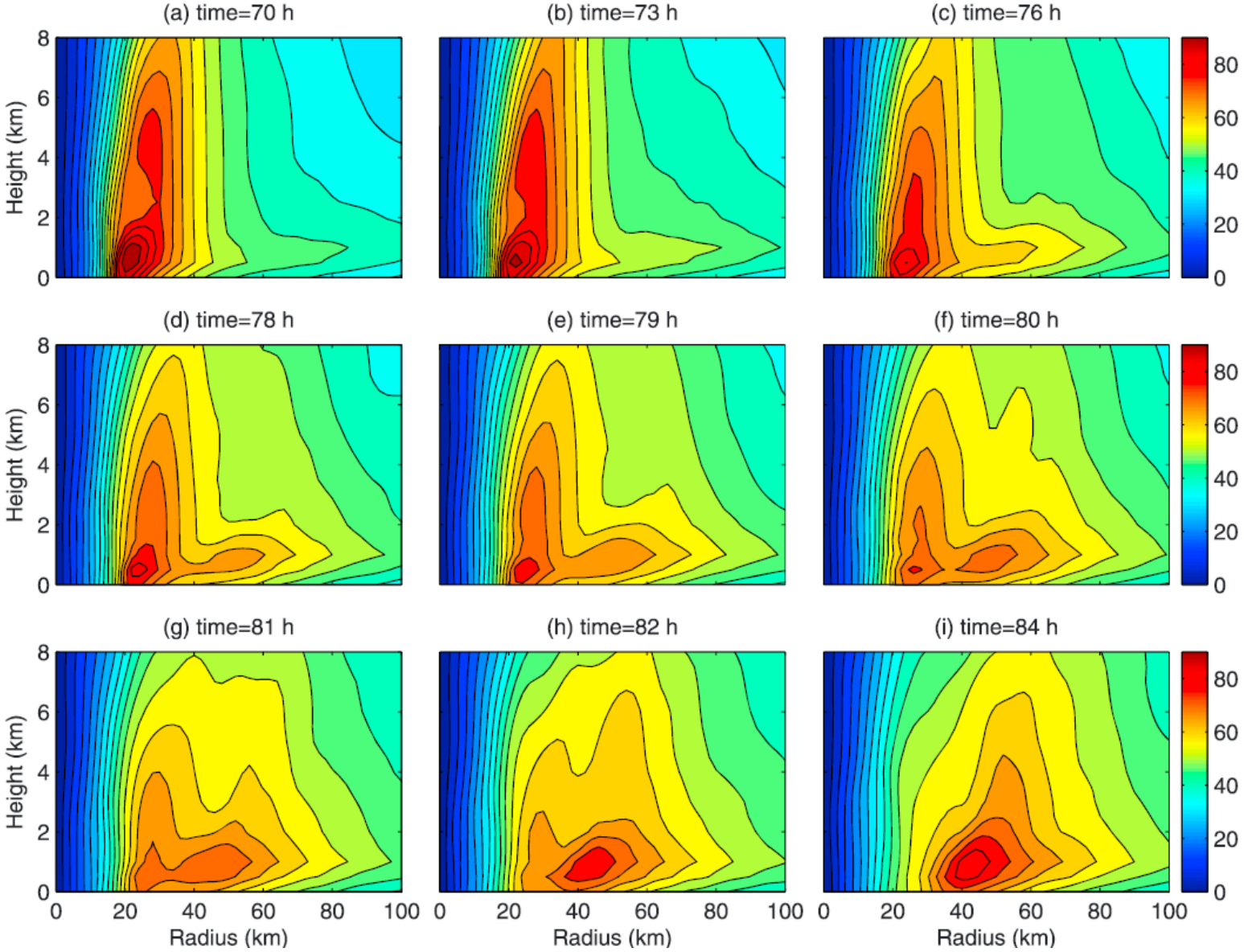

Interaction between eyewalls & RB during ERC

S-E diagnose with outer rainband heating only

contour: w < 0
color: diabatic heating

w at the inner eyewall: 0.03 m/s

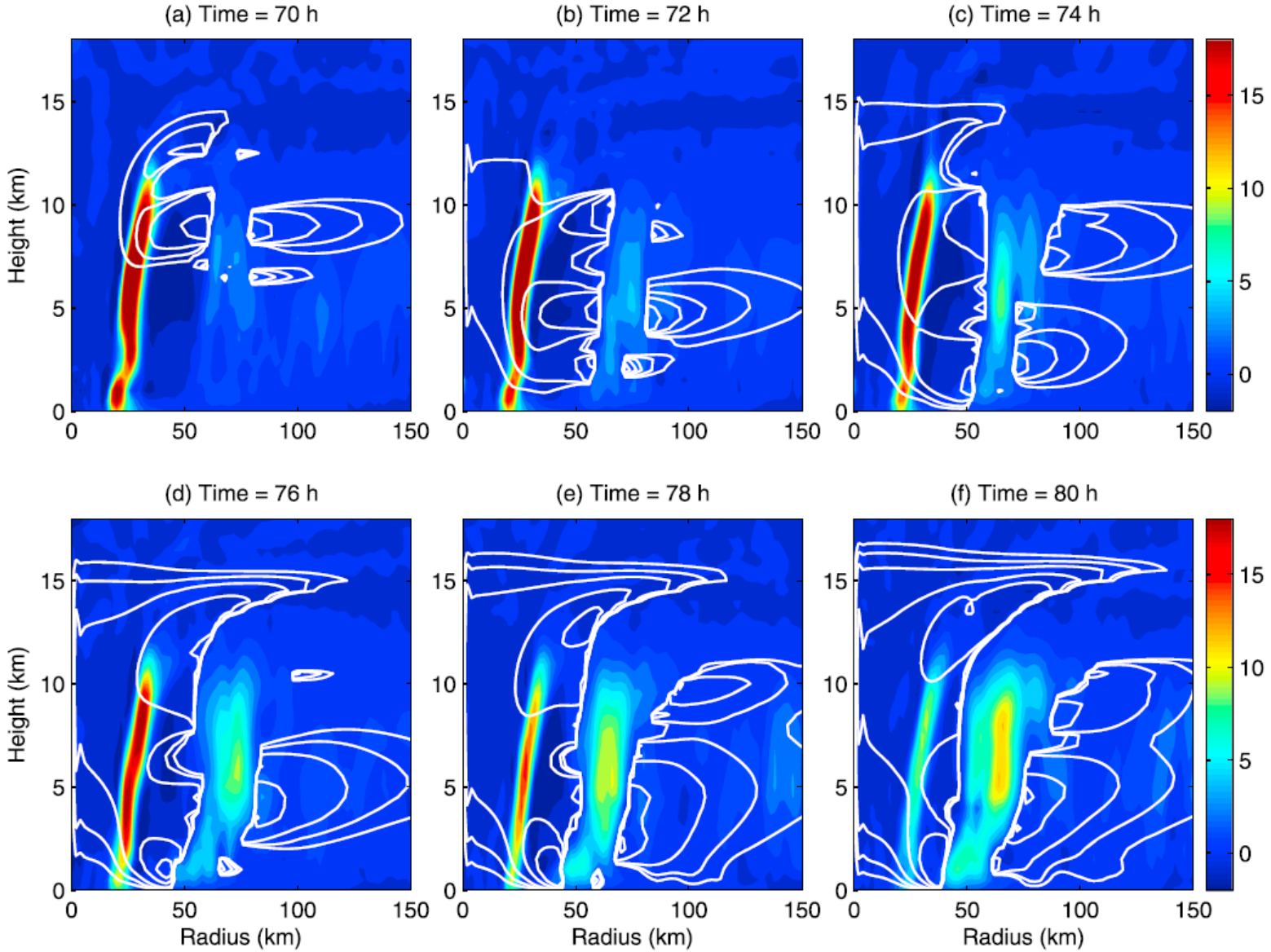

Interaction between eyewalls & RB during ERC

S-E diagnose with inner eyewall heating only

contour: w < 0
color: diabatic heating

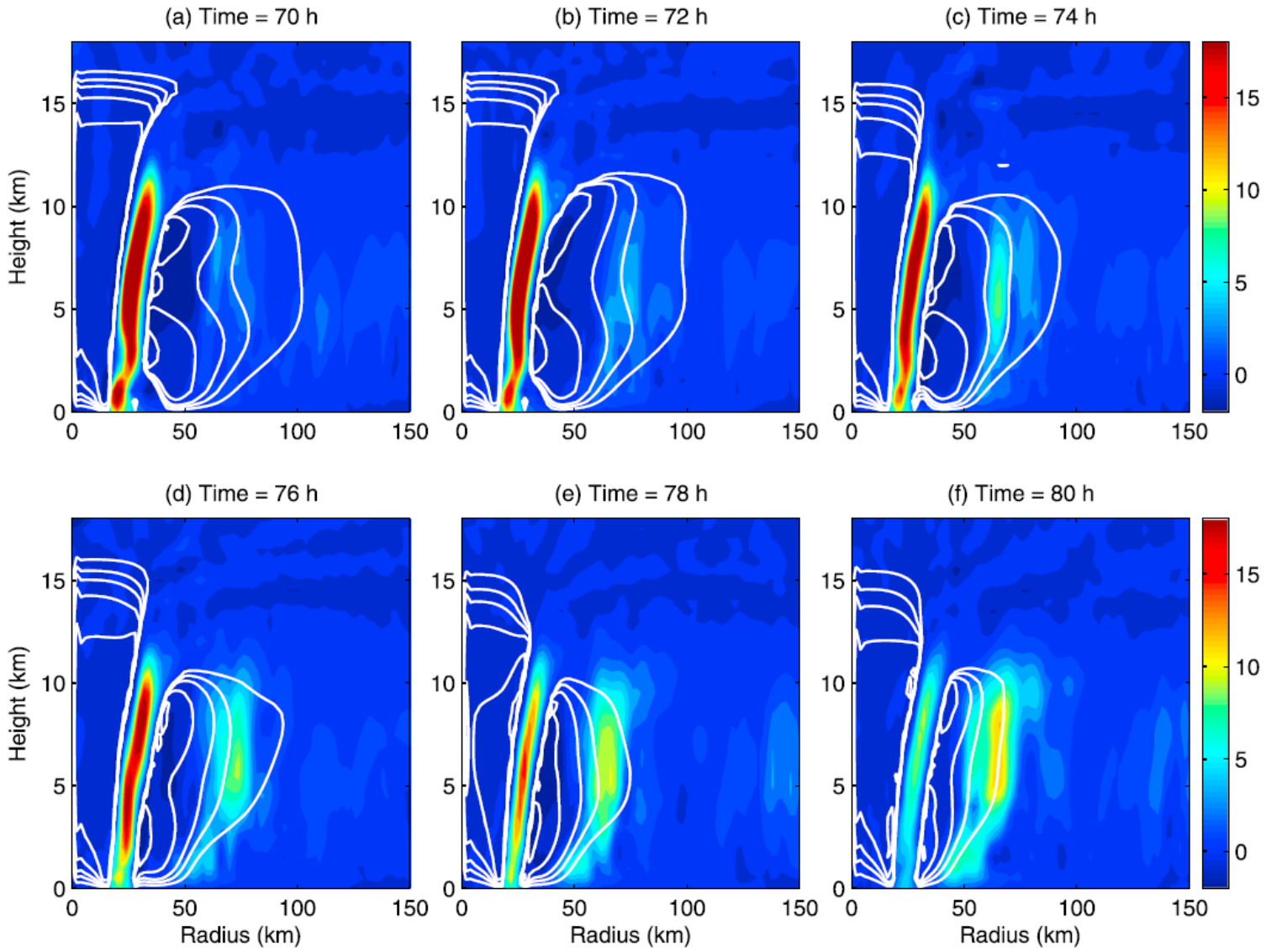

Interaction between eyewalls & RB during ERC

S-E diagnose with heating and momentum forcing

contour: u
  white: by outer rainband
  black: by eyewall

color: diabatic heating

——— u < 0
..... u > 0

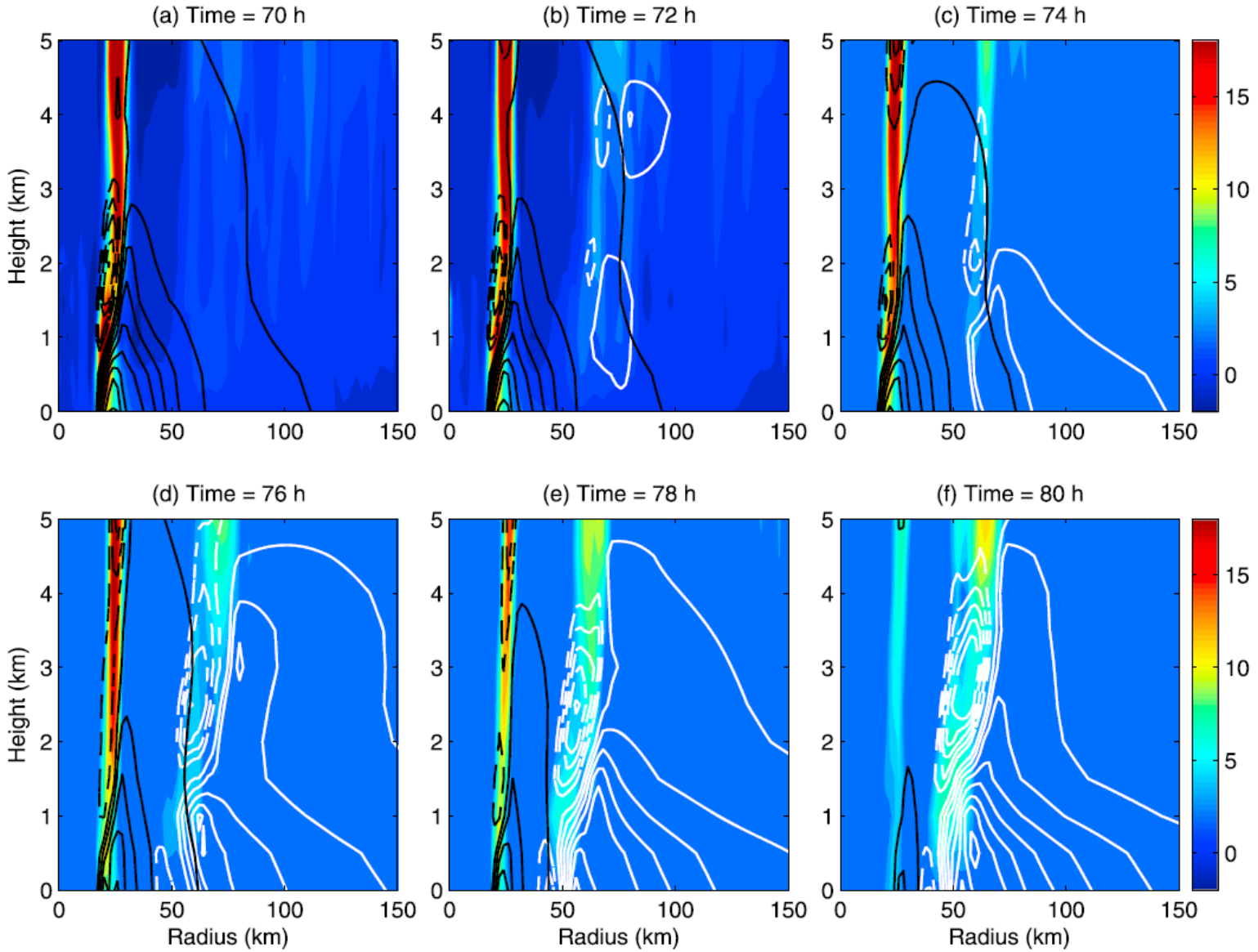

Summary

- This paper used 3D full-physics WRF simulation to investigate the role of rainband convection in SEF and ERC and physical processes of secondary wind maximum.

- From the tangential momentum analysis, the positive tendency of tangential wind at the SEF region was contributed by grid-resolved processes, which was dominated by axisymmetric advections.

- The Sawyer-Eliassen diagnoses indicated that only the heating from outer rainband convection can induce large positive tangential wind tendency. The outer rainband heating must reach 10% of the eyewall heating, so that it can initiate and drive the secondary tangential wind maximum.

Summary

- The mechanism for the development of outer rainband convection:
  1. Sporadic convection occurs in the outer rainband region at mid-level.
  2. The convergence of $\bar{u}$ and acceleration of $\bar{v}$ are generated at the convection base.
  3. The moisture increases in the lower level.
  4. Convection occurs at lower level.

- The outer rainband (eyewall) heating induced subsidence over the eyewall (outer rainband) region. Only the inner eyewall dissipated.

- The outflow induced by outer rainband heating canceled out the inflow induced by eyewall heating. When the outer rainband got stronger, the associated outflow extended vertically to cutoff the inflow to the eyewall.